ARTICLE

Journal of Materials Chemistry
www.rsc.org/materials

Conducting oriented-$[(n\text{-}C_4H_9)_4N]_2[Ni(dcbdt)_2]_5$ and new (BEDT-TTF)$[Ni(dcbdt)_2]$ phases as microcrystalline films, electrodeposited on silicon substrates

Dominique de Caro,*[a] Helena Alves,[b] Manuel Almeida,*[b] Sylvain Caillieux,[a] Mohamed Elgaddari,[a] Christophe Faulmann,[a] Isabelle Malfant,[a] François Senocq,[c] Jordi Fraxedas,[d] Antoine Zwick[e] and Lydie Valade*[a]

[a]*Laboratoire de Chimie de Coordination (CNRS UPR 8241), 205, route de Narbonne, 31077 Toulouse Cedex 4, France. E-mail: decaro@lcc-toulouse.fr Fax: +33 (0)5-61-55-30-03; Tel: +33 (0)5-61-33-31-37*

[b]*Departamento de Química, Instituto Tecnológico Nuclear Estrada National no. 10, 2685-953 Sacavém, Portugal. E-mail: malmeida@itn.pt*

[c]*ENSIACET-CIRIMAT (CNRS UMR 5085), 118, route de Narbonne, 31062 Toulouse Cedex 4, France*

[d]*Institut de Ciència de Materials de Barcelona (CSIC), Campus de la UAB, 08193 Bellaterra, Spain*

[e]*Laboratoire de Physique des Solides (CNRS UMR 5477), 118, route de Narbonne, 31062 Toulouse Cedex 4, France*

Received 23rd April 2004, Accepted 29th June 2004
First published as an Advance Article on the web 9th August 2004

$Ni(dcbdt)_2$-based molecular materials, namely $[(n\text{-}C_4H_9)_4N]_2[Ni(dcbdt)_2]_5$, and (BEDT-TTF)$[Ni(dcbdt)_2]$ have been processed as microcrystalline films on (001)-oriented silicon substrates using the electrodeposition technique [$dcbdt^{2-}$: 4,5-dicyanobenzene-1,2-dithiolato; BEDT-TTF: bis(ethylenedithio)tetrathiafulvalene]. Electrodeposited $[(n\text{-}C_4H_9)_4N]_2[Ni(dcbdt)_2]_5$ is made of thin platelets. Elemental analysis and X-ray photoelectron spectroscopy data are in agreement with a 2 : 5 stoichiometry. X-Ray powder diffraction measurements indicate that the growth is highly anisotropic, the *ab*-plane being parallel to the silicon surface. The films exhibit a semiconducting behaviour with a room-temperature conductivity of about 1.2×10^{-2} S cm^{-1}. Electrodeposition run in the presence of the BEDT-TTF donor molecule leads to faceted microcrystals (size: 5–100 μm) of (BEDT-TTF)$[Ni(dcbdt)_2]$ as evidenced by scanning electron microscopy. Single crystal data show that this new (BEDT-TTF)$[Ni(dcbdt)_2]$ phase is isostructural to the previously described (BEDT-TTF)$[Au(dcbdt)_2]$. Again, elemental analysis and X-ray photoelectron spectroscopy data are in agreement with a 1 : 1 stoichiometry. The room-temperature conductivity of the film is about 3×10^{-6} S cm^{-1}. This low value is comparable to that measured on (BEDT-TTF)$[Au(dcbdt)_2]$ single crystals. For both materials the charge transfer is similar, as consistently evaluated from Raman, infrared and photoemission measurements.

Introduction

Molecule-based materials exhibit interesting transport properties (metallic, semiconducting, superconducting) as well as magnetic properties related to their dimensionality and hence have become the subject of intense research interest.[1] However, it is difficult to envision a technological breakthrough by using them in the usual single crystal form. Preparation as thin films offers an attractive alternative to overcome this difficulty, and encouraging results have actually been emerging during the past 20 years. Up to this date, reported efforts to prepare thin films of metallic, semiconducting and magnetic materials have made use of different techniques, such as thermal sublimation in a high vacuum,[2–6] chemical vapour deposition,[7–10] Langmuir–Blodgett techniques,[11] halide evaporation on an organic donor-treated polymer film,[12] adsorption in solution[10] and electrodeposition.[10,13–16] For gas phase techniques such as sublimation in high vacuum and chemical vapour deposition, precursors should fit specific physical and chemical criteria (volatility, transport in the gas phase without decomposition). These methods, involving a gas–surface reaction, lead to a better homogeneity of the deposit in terms of coverage and thickness. In techniques based on the use of solutions of the precursor molecules, such as adsorption in solution and electrodeposition, the chemical criteria are more familiar to chemists (solubility, stability in organic solution, *etc.*). Concerning thin films of molecule-based compounds containing bis(dithiolene) transition metal complexes as building blocks, adsorption in solution and electrodeposition techniques have been successfully applied. Examples are thin $[(n\text{-}C_4H_9)_4N]_{0.9}$-$[Ni(dmid)_2]$ films ($dmid^{2-}$: 1,3-dithiole-2-one-4,5-dithiolato) electrodeposited on a platinum electrode by applying galvanostatic conditions[14] and $TTF[Ni(dmit)_2]_2$ ($dmit^{2-}$: 1,3-dithiole-2-thione-4,5-dithiolato).[10,17] When prepared by electrodeposition on silicon substrates the $TTF[Ni(dmit)_2]_2$ films are conductive at room temperature and remain metallic down to 14 K.[17]

Recently, the synthesis of $M(dcbdt)_2$ complexes ($dcbdt^{2-}$: 4,5-dicyanobenzene-1,2-dithiolato, Scheme 1) opened the route to a novel family of molecule-based conductors.[18,19] The presence of a relatively large and extended π-system within the dcbdt ligand makes the complexes relatively easy to oxidise and, for M = Ni and Au, the partially oxidised species $[(n\text{-}C_4H_9)_4N]_2[M(dcbdt)_2]_5$ were obtained by electrocrystallisation.[20,21] In this paper, we describe the electrodeposition of the previously known $[(n\text{-}C_4H_9)_4N]_2[Ni(dcbdt)_2]_5$ phase, and of the new (BEDT-TTF)$[Ni(dcbdt)_2]$ charge transfer complex [BEDT-TTF: bis(ethylenedithio)tetrathiafulvalene, Scheme 2] on silicon wafers.

DOI: 10.1039/b406122e

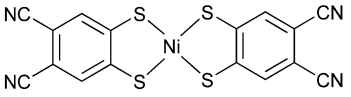

Scheme 1 The bis(4,5-dicyanobenzene-1,2-dithiolato)nickel complex.

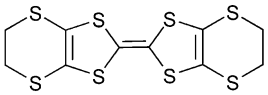

Scheme 2 The donor BEDT-TTF.

Experimental

Intrinsic Si(001) wafers (one face polished) were purchased from Siltronix (diameter: 5 cm; thickness: 275 μm; conductivity at room temperature *ca.* 10^{-3} S cm^{-1}). The wafers are stripped in an NH_4F/HF solution (12.5% HF at 50% and 87.5% NH_4F at 40%) and then washed in distilled water before use. Electrodeposition experiments are carried out using intrinsic Si(001) as the anode and a platinum wire as the cathode. BEDT-TTF was purchased from Aldrich.

Electrodeposition of $[(n\text{-}C_4H_9)_4N]_2[Ni(dcbdt)_2]_5$ was carried out on an entire silicon wafer (diameter: 5 cm). Typically, a solution of $[(n\text{-}C_4H_9)_4N][Ni(dcbdt)_2]$ (112 mg) in freshly distilled and degassed CH_2Cl_2 (230 mL) is introduced into a Schlenk-type cylindrical one-compartment (400 mL) electrochemical cell. The galvanostatic oxidation is performed at room temperature and at a current density of 0.5 μA cm^{-2}. Within a day, microcrystals appear and grow homogeneously on the Si surface. A *ca.* 10 μm continuous and adherent microcrystalline film is obtained after a four day electrolysis duration.

Electrodeposition of (BEDT-TTF)$[Ni(dcbdt)_2]$ was performed on rectangular-shaped silicon substrates (0.5 × 1.5 cm^2). Typically, a solution of BEDT-TTF (2 mg) and $[(n\text{-}C_4H_9)_4N][Ni(dcbdt)_2]$ (10 mg) in freshly distilled and degassed CH_2Cl_2 (12 mL) is introduced into the anodic compartment of an H-type electrochemical cell. A solution of $[(n\text{-}C_4H_9)_4N][Ni(dcbdt)_2]$ (10 mg) in CH_2Cl_2 (12 mL) is introduced into the cathodic compartment where it will only act as the supporting electrolyte. The oxidation of the BEDT-TTF organic donor is performed at constant current (1 μA) at room temperature in the presence of the $[Ni(dcbdt)_2]^-$ complex. Within two days, a black deposit (thickness ≈ 10 μm) is obtained on the silicon electrode. We have observed that composition, microstructure and spectroscopic properties of the films remain unchanged after several months of exposure to air. However, their adherence on Si substrates is lowered.

Elemental analyses were performed by the Microanalysis Service of LCC-CNRS. Scanning electron micrograph (SEM) images were obtained on a Jeol Model JSM 840A microscope. Infrared spectra were recorded (in a KBr matrix) on a sample of the film peeled off from the Si surface, using a Perkin-Elmer Spectrum GX spectrophotometer. The Raman measurements were performed using a DILOR XY micro-Raman set-up. The spectra are obtained at room temperature using the 647 nm line of a Kr laser. The incident beam is focused onto the film through the ×100 microscope objective, giving a spot size of *ca.* 1 μm^2. The back-scattered light is collected through the same objective, dispersed and then imaged onto a CCD detector. Using a laser power density of about 10^5 W cm^{-2}, no major degradation of the material appears. X-Ray diffraction data for the $[(n\text{-}C_4H_9)_4N]_2[Ni(dcbdt)_2]_5$ film were collected with a Seifert XRD 3000 TT, using the Cu Kα radiation (1.5418 Å), fitted with a diffracted beam monochromator. The diffractometer is in the Bragg–Brentano configuration (θ/θ). X-Ray diffraction data for (BEDT-TTF)$[Ni(dcbdt)_2]$ single crystals collected from an edge of the Si substrate were taken using an Xcalibur diffractometer (Oxford Diffraction) equipped with a sealed Mo Kα (λ = 0.71073 Å) X-ray source. XPS spectra were acquired with an EA10P hemispherical analyser (SPECS) using non-monochromatized Al Kα radiation. Conductivity measurements of the $[(n\text{-}C_4H_9)_4N]_2[Ni(dcbdt)_2]_5$ film were performed using the standard four-probe method between room temperature and 185 K. Electrical contacts between the gold wires and the film are made by using gold paint. They are drawn parallel to each other keeping a large inter-wire distance (2.2 mm). The room-temperature conductivity of the (BEDT-TTF)$[Ni(dcbdt)_2]$ thin film was evaluated on a compressed pellet of the product collected from the substrate surface.

Results and discussion

Microcrystalline films of $[(n\text{-}C_4H_9)_4N]_2[Ni(dcbdt)_2]_5$

$[(n\text{-}C_4H_9)_4N]_2[M(dcbdt)_2]_5$ (M = Ni, Au) single crystals can be prepared as thin plates (3 × 0.3 × 0.05 mm) on the surface of a platinum anode, by electrocrystallisation from the corresponding $[(n\text{-}C_4H_9)_4N][M(dcbdt)_2]$ complex under galvanostatic conditions (*ca.* 0.2 μA cm^{-2}).[20] Both compounds present a triclinic structure ($P\bar{1}$) showing stacks of pentamerised $M(dcbdt)_2$ units along [−2 1 0]. The electrical conductivity measured along the long axis [−2 1 0] of the elongated-shaped crystals denotes a semiconducting behaviour (σ_{RT} = 0.13 S cm^{-1} and E_a = 0.176 eV for M = Ni; σ_{RT} = 10 S cm^{-1} and E_a = 0.027 eV for M = Au).

Microcrystalline films of $[(n\text{-}C_4H_9)_4N]_2[Ni(dcbdt)_2]_5$ are obtained by electrolysis on a silicon wafer in a one-compartment cell containing a dichloromethane solution of $[(n\text{-}C_4H_9)_4N][Ni(dcbdt)_2]$. The film mainly forms on the non-polished face of the silicon electrode. Elemental analysis of a sample of film scratched from the surface gives the following results: %C = 49.90; %H = 2.77; %N = 11.05. These values are in good agreement with the data calculated for $[(n\text{-}C_4H_9)_4N]_2[Ni(dcbdt)_2]_5$ (%C = 50.18; %H = 3.46; %N = 11.49). Therefore, the same 2 : 5 stoichiometry is obtained within the films, as on $[(n\text{-}C_4H_9)_4N]_2[Ni(dcbdt)_2]_5$ single crystals. Electron micrographs evidence that the film is made of thin platelets (30–55 μm long, 1–8 μm width, thickness < 1 μm) randomly distributed on the substrate surface (Fig. 1). This morphology is in sharp contrast with the dendritic growth reported for $[(n\text{-}C_4H_9)_4N]_{0.9}[Ni(dmid)_2]$ on a Pt metal foil[14] and also for $[(n\text{-}C_4H_9)_4N]_2[Ni(dcbdt)_2]_5$ platelets on platinum wires, both at high current densities (*i.e.* 25 μA cm^{-2}). As a matter of fact, in our case, much lower current densities (0.5 μA cm^{-2}) are applied and could favour the growth of long platelets or needles. A SEM side view of a segment of the film peeled off from the surface allows us to evaluate the thickness at *ca.* 10 μm.

Raman spectra performed on the film [Fig. 2(a)] and on the precursor material [Fig. 2(b)] exhibit almost the same characteristic vibrational bands. However, signal-to-noise is slightly better for the starting $[(n\text{-}C_4H_9)_4N][Ni(dcbdt)_2]$ microcrystalline powder. Bands at 405(m), 362(s) and 347(s) cm^{-1} are

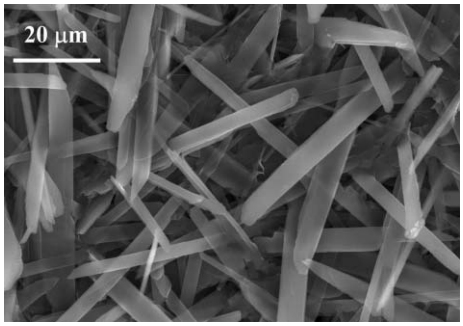

Fig. 1 SEM image of the deposit of $[(n\text{-}C_4H_9)_4N]_2[Ni(dcbdt)_2]_5$.

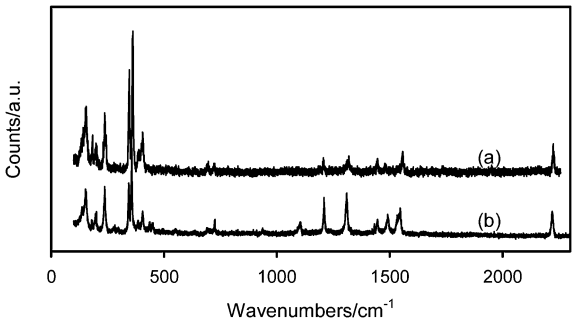

Fig. 2 Raman spectra of the deposit of $[(n\text{-}C_4H_9)_4N]_2[Ni(dcbdt)_2]_5$ (a) and of the starting $[(n\text{-}C_4H_9)_4N][Ni(dcbdt)_2]$ complex (b).

respectively assigned to C–S stretching, Ni–S stretching, and out-of-phase deformation of the 5-membered rings connected to the nickel.[22,23] It should be noted that medium intensity Raman signals appearing at 1546 cm^{-1} (aromatic C=C stretching modes) and 2220 cm^{-1} (CN stretching modes) for the precursor compound shift to higher frequencies, that is 1557 and 2225 cm^{-1}, respectively, for the film. This frequency shift is in agreement with the decrease of the average value of the charge of the $Ni(dcbdt)_2$ moiety $[Ni(dcbdt)_2^{-} \rightarrow Ni(dcbdt)_2^{0.4-}]$, as previously reported in the case of thin films of $[(n\text{-}C_4H_9)_4N]_{0.9}[Ni(dmid)_2]$.[14] The other medium intensity Raman signals observed in the spectrum are 1206, 1319, and 1445 cm^{-1}. From infrared spectra and also due to the charge change of the complex in the deposit relatively to $[Ni(dcbdt)_2]^{-}$, carbon–hydrogen stretching vibrations of the phenyl groups are shifted from 3061 cm^{-1} in the starting complex to 3067 cm^{-1} in the film. As expected, CH stretching modes of butyl groups of the $[(n\text{-}C_4H_9)_4N]^{+}$ cations (2850–2965 cm^{-1}) remain unchanged after partial oxidation of $[(n\text{-}C_4H_9)_4N][Ni(dcbdt)_2]$. The nitrile vibration modes are present at 2226 cm^{-1} in the infrared spectrum of the deposit, a value almost identical to that observed in the Raman spectrum.

The powder diffraction data of the film show a highly oriented film (Fig. 3). The refinement of the collected data gave the following crystallographic data: $a = 7.999(8)$, $b = 17.271(2)$, $c = 22.490(3)$ Å, $\alpha = 69.01(1)$, $\beta = 89.08(1)$, $\gamma = 78.90(1)^{\circ}$, to be compared with $a = 8.000(1)$, $b = 17.288(3)$, $c = 22.490(4)$ Å, $\alpha = 69.181(8)$, $\beta = 89.161(12)$, $\gamma = 78.14(1)^{\circ}$ obtained from a single crystal study.[20] The very good agreement of the lattice parameters confirms the 2 : 5 stoichiometry and shows that the deposition process does not affect the structural arrangement of the compound although the very weak intensity of the diffraction lines other than (001) and (002) may limit the precision of the measurement. The growth of the film is highly anisotropic, the *ab*-plane being parallel to the wafer surface. According to

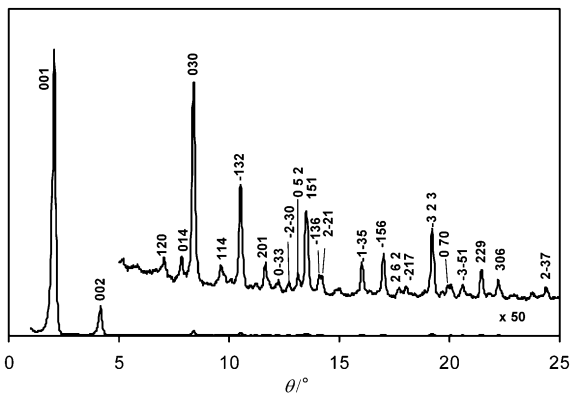

Fig. 3 X-Ray diffraction pattern of electrodeposited $[(n\text{-}C_4H_9)_4N]_2[Ni(dcbdt)_2]_5$.

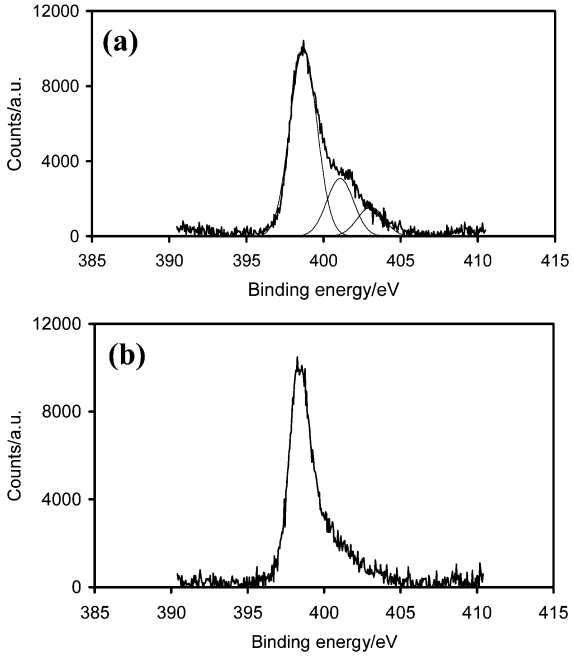

Fig. 4 X-Ray photoelectron spectra of the N 1s line for: (a) thin $[(n\text{-}C_4H_9)_4N]_2[Ni(dcbdt)_2]_5$ films, and (b) thin (BEDT-TTF)$[Ni(dcbdt)_2]$ films.

the Scherrer relation, the mean thickness of the elementary crystals along the direction perpendicular to the *ab*-plane has been estimated to be 280 ± 15 Å.

Fig. 4(a) shows the XPS spectrum of the N 1s line. The main peak in Fig. 4(a) is located at a 398.7 eV binding energy, which arises from the cyano contribution of $Ni(dcbdt)_2$. The 401.7 eV shoulder corresponds to the tetrabutylammonium contribution as inferred by comparing with the N 1s line from (BEDT-TTF)$[Ni(dcbdt)_2]$, Fig. 4(b), where tetrabutylammonium is indeed absent. The nominal sulfur to nitrogen ratio (20/22 = 0.91) is in reasonable agreement with the surface 1.2 ratio derived from the S 2p and N 1s signals. The binding energy of the cyano-based line of neutral TCNQ is 399.8 eV and shifts to lower binding energies when charge is transferred (398.0 eV for a charge transfer of 0.59 as in [TTF][TCNQ]).[5] A simple extrapolation of the 398.7 eV value based on these two TCNQ values would give a charge transfer of 0.4, in agreement with the Raman shifts discussed above. Moreover, the main peak of the Ni 2p XPS spectrum corresponds to the Ni $2p_{3/2}$ component (854.1 eV) with a spin–orbit splitting of 17.2 eV. Shake-up satellites are found at about 8 eV from the main peaks. The electronic origin of the main line and satellite (relative contribution from d^8, d^9L and $d^{10}L^2$ states) has not yet been investigated but the XPS spectrum closely resembles those found for NiS_2.[24]

The electrical conductivity of $[(n\text{-}C_4H_9)_4N]_2[Ni(dcbdt)_2]_5$ microcrystalline films is about 1.2×10^{-2} S cm^{-1} at room temperature and follows a thermally activated semiconducting behaviour. The plot of $\log(\sigma)$ *versus* $1/T$ shows an activation energy of 157 meV in the 295–230 K range (Fig. 5). This value is reduced to 67 meV below 230 K. Remarkably, a nearly identical semiconducting behaviour was observed on $[(n\text{-}C_4H_9)_4N]_2[Ni(dcbdt)_2]_5$ single crystals with very similar activation energy values (176 meV at high temperatures and 68 meV below 250 K).[18] The origin of this noticeable change in the activation energy is not yet clear and may be associated to a phase transition. The room-temperature conductivity of the film is one order of magnitude lower than that of single crystals (0.15 S cm^{-1}). The [−2 1 0] direction, which is the stacking direction and the direction of highest conductivity, also corresponds to the direction of the long axis of the needle-like crystals.[21] As electron micrographs show that the grown

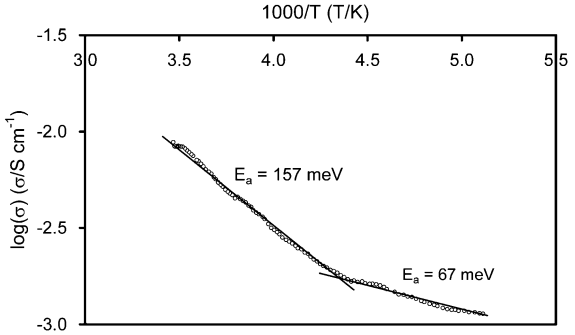

Fig. 5 Conductivity as a function of reciprocal temperature for electrodeposited $[(n\text{-}C_4H_9)_4N]_2[Ni(dcbdt)_2]_5$.

needles lay on the surface (Fig. 1), the direction of highest conductivity is part of the plane in which the film conductivity is measured. This feature, the contributions of other directions within the crystallites, and the polycrystalline nature of the film, which generates grain boundaries, account for the lower conductivity value of the film *versus* that of the crystal.

Microcrystalline films of (BEDT-TTF)[Ni(dcbdt)$_2$]

Microcrystalline films of (BEDT-TTF)[Ni(dcbdt)$_2$] are fabricated by galvanostatic electrolysis on a rectangular-shaped silicon substrate using a H-type electrochemical cell containing dichloromethane solutions of BEDT-TTF and $[(n\text{-}C_4H_9)_4N]$-[Ni(dcbdt)$_2$]. A black deposit forms on both polished and non-polished faces of the silicon electrode. It consists of faceted microcrystals (size: 5–100 μm; thickness: 1–10 μm) uniformly covering the substrate surface (Fig. 6).

Single crystals removed from the surface correspond to the new (BEDT-TTF)[Ni(dcbdt)$_2$] phase,† which is found to be isostructural with (BEDT-TTF)[Au(dcbdt)$_2$].[25] The asymmetric unit of (BEDT-TTF)[Ni(dcbdt)$_2$] contains one half BEDT-TTF unit and one half [Ni(dcbdt)$_2$] unit, with the centre of the central C=C bond and the Ni atoms placed on a centre of inversion (Fig. 7, top). Both molecules are planar, except the terminal ethylene groups of the BEDT-TTF, which adopt a staggered conformation (Fig. 7, bottom). (BEDT-TTF) molecules and [Ni(dcbdt)$_2$] units are parallel to each other and form alternated stacks along the [1 1 0] direction. The structure can be regarded as sheets of (BEDT-TTF) molecules and sheets of

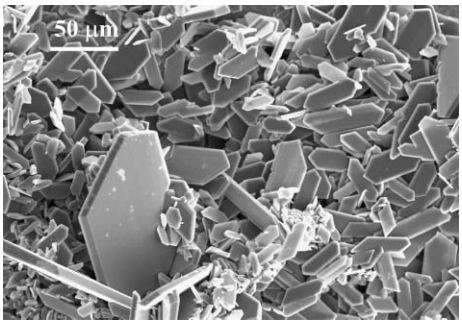

Fig. 6 SEM image of electrodeposited thin films of (BEDT-TTF)[Ni(dcbdt)$_2$].

† Chemical formula: $C_{26}H_{12}N_4NiS_{12}$ (M = 823.83), T = 180(2) K, a = 6.9335(7), b = 8.3487(11), c = 13.6785(18) Å, α = 101.919(11), β = 103.247(10), γ = 98.177(10) °, V = 739.02(16) Å^3, crystal system: triclinic, space group: $P\bar{1}$, Z = 1, linear absorption coefficient μ = 1.534 mm^{-1}, reflections collected: 8328, independent reflections: 4707 [R(int) = 0.0692], final R indices [$I > 2\sigma(I)$]: R_1 = 0.0458, wR_2 = 0.0569, R indices (all data): R_1 = 0.1332, wR_2 = 0.0732.
CCDC reference number 237448. See http://www.rsc.org/suppdata/jm/b4/b406122e/ for crystallographic data in .cif or other electronic format.

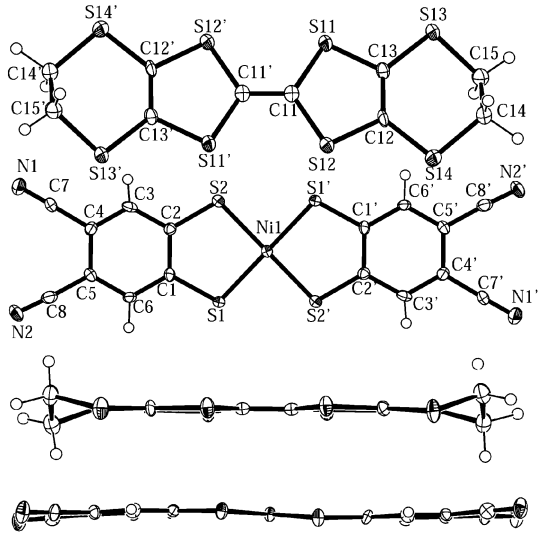

Fig. 7 Molecular structure of BEDT-TTF and Ni(dcbdt)$_2$ in (BEDT-TTF)[Ni(dcbdt)$_2$] (top: onto the plane of the molecules; bottom: side view of the molecules).

[Ni(dcbdt)$_2$] units lying in the (0 $\bar{2}$ 3) plane. The inter-planar distance between donor and acceptor molecules (or between sheets) is *ca.* 3.60 Å. Within the donor sheet, BEDT-TTF units are connected to each other through two short S···S contacts involving S13 and S14 (see Table 1), whereas no short contact exists within the acceptor sheet. (BEDT-TTF) units and [Ni(dcbdt)$_2$] units are connected to each other through short S···S contacts, either within a stack (S2···S12), or between adjacent stacks (S1···S12 and S2···S11). Such an alternate arrangement with so few contacts is in agreement with the low value of the conductivity observed on a compressed pellet (see below), as also reported for the gold analogue.[25]

The Raman spectrum of the films exhibits signals at 345(w), 356(w), 406(w), 1550(w), and 2224(w) cm^{-1}, whose assignments are identical to those given for the $[(n\text{-}C_4H_9)_4N]_2$-$[Ni(dcbdt)_2]_5$ complex. In the carbon–carbon double bond stretching region (Fig. 8), peaks at 1313(s), 1446(sh) and 1550(w) cm^{-1} are present, as in the Raman spectrum of $[Ni(dcbdt)_2]^-$. Additional strong signals at 1420 and 1450 cm^{-1} are ascribed to the central and peripheral C=C modes of BEDT-TTF (Fig. 8). For neutral BEDT-TTF, strong or medium C=C modes are observed in the 1494–1552 cm^{-1} range.[26] Lower C=C frequencies observed for the film are in agreement with the cationic character of the BEDT-TTF moiety. A similar frequency shift due to charge transfer between donor and acceptor molecules has been observed for thin films of TTF[Ni(dmit)$_2$]$_2$.[10,17] In the infrared spectrum of the films, carbon–hydrogen stretching vibrations of the phenyl groups are present at 3045 and 3068 cm^{-1}, and CH_2 stretching

Table 1 Contacts for (BEDT-TTF)[Ni(dcbdt)$_2$]

	Atom 1	Atom 2	Symmetry operation[a]	Length/Å
Intra-sheet: donor–donor	S13	S14	$-1 + x, y, z$	3.626
Inter-sheet: inter-stack (donor–acceptor)	S1	S12	$-1 + x, y, z$	3.627
Inter-sheet: inter-stack (donor–acceptor)	S11	S2	$x, 1 + y, z$	3.642
Inter-sheet: intra-stack (donor–acceptor)	S2	S12	$1 - x, 1 - y, -z$	3.692

[a] Symmetry operation to be applied on the second atom.

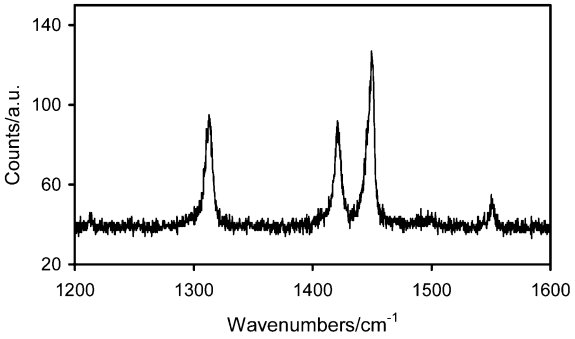

Fig. 8 Raman spectrum of electrodeposited thin films of (BEDT-TTF)[Ni(dcbdt)$_2$] (ν_{CC} region).

modes of BEDT-TTF are in the 2850–2980 cm^{-1} range. Finally, the nitrile vibration modes are present at 2224 cm^{-1} in the infrared spectrum of the deposit, a value identical to that observed in the Raman spectrum.

Photoelectron spectra of the films evidence a N 1s signal located at 398.4 eV [Fig. 4(b)]. This position corresponds to the charge transferred to the Ni(dcbdt)$_2$ moiety and the result indicates that this quantity should be essentially the same for both compounds, [N(n-C$_4$H$_9$)$_4$]$_2$[Ni(dcbdt)$_2$]$_5$ and (BEDT-TTF)[Ni(dcbdt)$_2$]. This is in agreement with the Raman and infrared data: the nitrile mode is located at 2224 cm^{-1} for both deposits, while this mode is at 2220 cm^{-1} for the starting [(n-C$_4$H$_9$)$_4$N][Ni(dcbdt)$_2$]. The asymmetry of the N 1s peak at higher binding energies should arise from shake-up satellites, related to the HOMO–LUMO gap. The experimental sulfur to nitrogen ratio obtained from XPS is 3.2, as evaluated from the S 2p and N 1s signals, which is in good agreement with the nominal 12/4 = 3 ratio. This result indicates that the 1 : 1 stoichiometry found within the bulk by X-ray crystal data is similar to that found on the surface.

The room-temperature conductivity, evaluated on a compressed pellet of the film collected from the silicon surface, is about 3×10^{-6} S cm^{-1}. This low value is similar to that obtained on (BEDT-TTF)[Au(dcbdt)$_2$] single crystals ($<10^{-5}$ S cm^{-1}), and is consistent with the structural arrangement of the compound.[25]

Conclusion

We have reported on the growth of [Ni(dcbdt)$_2$]-based compounds as microcrystalline films on silicon wafers, a preliminary step towards the use of such molecular materials in future electronic devices. We have shown the feasibility of processing films of two systems, namely the [(n-C$_4$H$_9$)$_4$N]$_2$[Ni(dcbdt)$_2$]$_5$ phase, and a new charge transfer complex (BEDT-TTF)[Ni(dcbdt)$_2$]. The deposits have been characterized by various techniques, including scanning electron microscopy, powder or single crystal X-ray diffraction, photoelectron spectroscopy, and vibrational spectroscopies (Raman and infrared). Transport measurements have also been carried out. [(n-C$_4$H$_9$)$_4$N]$_2$[Ni(dcbdt)$_2$]$_5$ thin films behave as semiconductors ($\sigma_{300\ K} \approx 1.2 \times 10^{-2}$ S cm^{-1}). (BEDT-TTF)[Ni(dcbdt)$_2$] films show low conductivity ($\sigma_{300\ K} \approx 3 \times 10^{-6}$ S cm^{-1}). Although conductivity values are low, Ni(dcbdt)$_2$-based films are easy to process, are adherent onto the silicon surface and can be produced without a change in their physical properties.

Within the molecule-based materials field, one can regret that, since the 1970s the ever-growing number of chemical systems, and the wide variety of associated physical properties, has not been accompanied with a similarly intense progress in terms of processing. It appears that this field has remained too close to academic chemical or physical studies. Therefore, a lot remains to be done to envision a technological breakthrough within this domain.

Acknowledgements

The authors gratefully thank V. Collière for SEM micrographs. D. Bérail, from Motorola, is acknowledged for supplying supports for conductivity measurements. This work has been carried out within the frame of the COST D14/003/99 programme (CNRS-LCC Toulouse and ITN Sacavém). The work in Portugal was partially supported by FCT under contract POCTI 35452/99.

References

1 J. Fraxedas, *Adv. Mater*, 2002, **14**, 1603 and refs. cited therein.
2 P. Chaudhari, B. A. Scott, R. B. Laibowitz, Y. Tomkiewicz and J. B. Torrance, *Appl. Phys. Lett.*, 1974, **24**, 439.
3 J. Moldenhauer, H. Wachtel, D. Schweitzer, B. Gompf, W. Eisenmenger, P. Bele, H. Brunner and H. J. Keller, *Synth. Met.*, 1995, **70**, 791.
4 M. Kilitziraki, A. J. Moore, M. C. Petty and M. R. Bryce, *Thin Solid Films*, 1998, **335**, 209.
5 J. Fraxedas, S. Molas, A. Figueras, I. Jiménez, R. Gago, P. Auban-Senzier and M. Goffman, *J. Solid State Chem.*, 2002, **168**, 384.
6 S. Molas, C. Coulon and J. Fraxedas, *CrystEngComm*, 2003, **5**, 310.
7 J. Caro, J. Fraxedas and A. Figueras, *Chem. Vap. Deposition*, 1997, **3**, 263–269.
8 D. de Caro, J. Sakah, M. Basso-Bert, C. Faulmann, J.-P. Legros, T. Ondarçuhu, C. Joachim, L. Ariès, L. Valade and P. Cassoux, *C. R. Acad. Sci. Paris, Sér. IIc*, 2000, **3**, 675.
9 D. de Caro, M. Basso-Bert, J. Sakah, H. Casellas, J. P. Legros, L. Valade and P. Cassoux, *Chem. Mater.*, 2000, **12**, 587.
10 S. Caillieux, D. de Caro, L. Valade, M. Basso-Bert, C. Faulmann, I. Malfant, H. Casellas, L. Ouahab, J. Fraxedas and A. Zwick, *J. Mater. Chem.*, 2003, **13**, 2931.
11 T. Takahashi, K.-i. Sakai, T. Yumoto, T. Akutagawa, T. Hasegawa and T. Nakamura, *Thin Solid Films*, 2001, **393**, 7.
12 M. Mas-Torrent, E. Laukhina, C. Rovira, J. Veciana, V. Tkacheva, L. Zorina and S. Khasanov, *Adv. Funct. Mater.*, 2001, **11**, 299.
13 A. C. Hillier, J. Hossick Schott and M. D. Ward, *Adv. Mater.*, 1995, **7**, 409.
14 S. G. Liu, P. J. Wu, Y. Q. Liu and D. B. Zhu, *Mol. Cryst. Liq. Cryst.*, 1996, **275**, 211.
15 H. H. Wang, K. L. Stamm, J. P. Parakka and C. Y. Han, *Adv. Mater.*, 2002, **14**, 1193.
16 L. Pilia, I. Malfant, D. de Caro, F. Senocq, A. Zwick and L. Valade, *New J. Chem.*, 2004, **28**, 52.
17 D. de Caro, J. Fraxedas, C. Faulmann, I. Malfant, J. Milon, J.-F. Lamère, V. Collière and L. Valade, *Adv. Mater*, 2004, **16**, 835.
18 D. Simão, H. Alves, D. Belo, S. Rabaça, E. B. Lopes, I. C. Santos, V. Gama, M. T. Duarte, R. T. Henriques, H. Novais and M. Almeida, *Eur. J. Inorg. Chem.*, 2001, **12**, 3119.
19 H. Alves, D. Simão, I. C. Santos, V. Gama, R. T. Henriques, H. Novais and M. Almeida, *Eur. J. Inorg. Chem.*, 2004, **6**, 1318.
20 H. Alves, D. Simão, E. B. Lopes, D. Belo, V. Gama, M. T. Duarte, H. Novais, R. T. Henriques and M. Almeida, *Synth. Met.*, 2001, **120**, 1011.
21 H. Alves, I. C. Santos, E. B. Lopes, D. Belo, V. Gama, D. Simão, H. Novais, M. T. Duarte, R. T. Henriques and M. Almeida, *Synth. Met.*, 2003, **133**, 397.
22 H. L. Liu, D. B. Tanner, A. E. Pullen, K. A. Abboud and J. R. Reynolds, *Phys. Rev. B*, 1996, **53**, 10 557.
23 K. I. Pokhodnya, C. Faulmann, I. Malfant, R. Andreu-Solano, P. Cassoux, A. Mlayah, D. Smirnov and J. Leotin, *Synth. Met.*, 1999, **103**, 2016.
24 S. R. Krishnakumar and D. D. Sharma, *Phys. Rev. B*, 2003, **68**, 155 110.
25 H. Alves, D. Simão, I. C. Santos, E. B. Lopes, H. Novais, R. T. Henriques and M. Almeida, *Synth. Met.*, 2003, **135–136**, 543.
26 M. E. Kozlov, K. I. Pokhodnya and A. A. Yurchenko, *Spectrochim. Acta, Part A*, 1987, **43**, 323.